

Ultra-low Q_β value for the allowed decay of $^{110}\text{Ag}^m$ confirmed via mass measurements

J. Ruotsalainen,^{1,*} M. Stryjczyk,^{1,†} M. Ramalho,^{1,‡} T. Eronen,¹
Z. Ge,¹ A. Kankainen,¹ M. Mougeot,¹ and J. Suhonen^{1,2,§}

¹University of Jyväskylä, Department of Physics, Accelerator laboratory,
P.O. Box 35(YFL) FI-40014 University of Jyväskylä, Finland

²International Centre for Advanced Training and Research in Physics (CIFRA),
P.O. Box MG12, 077125 Bucharest-Măgurele, Romania

The mass of the electron-antineutrino can be determined in dedicated measurements of the β spectral shape near the β endpoint of a β^- transition, with a low Q value enhancing the sensitivity of the measurement. One such low- Q -value candidate is the transition between the 6^+ isomer of ^{110}Ag and the 5_2^+ state in ^{110}Cd ($Q_{\beta,m}^* = -0.12(131)$ keV). To reduce the uncertainty of the Q value, we have used the phase-imaging ion-cyclotron-resonance technique with the JYFLTRAP double Penning trap and performed a high-precision atomic-mass measurement of ^{109}Ag with ^{110}Cd as a reference. Combined with the known spectroscopic data, we obtain a re-evaluated value $Q_{\beta,m}^* = 405(135)$ eV, for the $^{110}\text{Ag}(6_m^+) \rightarrow ^{110}\text{Cd}(5_2^+)$ transition. This represents the lowest Q_β value for any allowed transition observed to date. In order to estimate the partial half-life ($t_{1/2}$) and branching ratio (Br) of the transition, nuclear shell-model calculations were performed using the $jj45pn$ Hamiltonian in combination with state-of-the-art atomic calculations. The computed values $t_{1/2} = 2.23^{+5.24}_{-1.28} \times 10^7$ years and $\text{Br} = 3.07^{+4.16}_{-2.15} \times 10^{-8}$, along with the thermal-neutron capture on stable ^{109}Ag as a viable production method, make $^{110}\text{Ag}^m$ a promising candidate for future antineutrino-mass measurements.

The determination of the absolute mass of neutrinos remains one of the big unanswered questions in physics. Currently, the most stringent limits come from the kinematic experiments: KATRIN [1, 2] and MARE [3, 4] for the electron antineutrino, and ECHo [5, 6] and HOLMES [7, 8] for the electron neutrino. They are based on the model-independent analysis of the end-point spectrum of β^- decays of ^3H (KATRIN) and ^{187}Re (MARE) or ^{163}Ho electron capture (ECHo and HOLMES). Another tritium-based experiment, Project 8, is currently being planned [9]. These three isotopes have been chosen due to the very small ground-state-to-ground-state Q_β values (18 592.071(22) eV for ^3H [10], 2863.2(6) eV for ^{163}Ho [11] and 2470.9(13) eV for ^{187}Re [12]). Nevertheless, despite such narrow energy windows, only a very small fraction of decays ends up near the endpoint, limiting the sensitivity of these experiments. In neutrino mass experiments involving β decay and electron capture (EC), a low Q value enhances sensitivity to (anti)neutrino mass. Thus, finding such decays with the smallest possible Q value is desirable for experiments aimed at determining the (anti)neutrino mass.

An alternative approach has been recently proposed where the decay proceeds to the excited nuclear state in the daughter isotope with an ultra-low Q^* value, usually < 1 keV [13]. The first promising β^- -decay candidate discovered is ^{115}In where the second-forbidden unique decay to the first excited states in ^{115}Sn ($9/2_{\text{gs}}^+ \rightarrow 3/2_1^+$) was experimentally observed [14, 15] and its Q_β^* value is around 200 eV [14, 16]. Two other β^- -decay isotopes of interest are ^{135}Cs where $Q_\beta^* = 0.44(31)$ keV for the first-forbidden unique decay to the excited $11/2^-$ state [17] as well as ^{131}I with the Q_β^* value of $1.03(23)$ keV for an al-

lowed decay to the excited $9/2^+$ state. [18]. Additionally, a promising EC candidate ^{159}Dy was recently discovered [19] with the Q_{EC}^* of $1.18(19)$ keV for the $^{159}\text{Dy}(3/2^-) \rightarrow ^{159}\text{Tb}^*(5/2^-)$ transition. However, with the exception of ^{115}In , these ultra-low- Q^* decays are still awaiting experimental confirmation.

While ^{115}In seems to be an ideal candidate for a new generation of neutrino-mass experiments, a small branching ratio ($\approx 10^{-6}$) resulting in a very long partial half-life ($\approx 10^{20}$ y [14]) is limiting its use. As a result, the search for other cases continues [19–30], with an emphasis on allowed transitions as they are the fastest and their β shape can be described analytically [31]. However, these studies are focused only on ground-state-to-excited-state decays [31], disregarding possible isomeric-state-to-excited-state (iso-ex) transitions.

One isomer that could be of interest for future antineutrino mass experiments is $^{110}\text{Ag}^m$ ($E_m = 117.59(5)$ keV, $J^\pi = 6^+$, $T_{1/2} \approx 250$ d [32, 33]). It decays predominantly (98.67(8)% via β^- to the excited states in stable ^{110}Cd (see Fig. 1), with a minor decay branch (1.33(8)% via internal transition [32, 33]. Additionally, it can be readily produced in nuclear reactors due to the large cross section (≈ 4.1 b) for thermal-neutron capture on stable ^{109}Ag [34, 35]. The literature $Q_\beta(^{110}\text{Ag}^m) \equiv Q_{\beta,m}$ value is $3008.3(13)$ keV [32, 36] and the recent studies constrained the excitation energy of the non-isomeric $^{110}\text{Cd}(5_2^+)$ state to $E_x = 3008.41(4)$ keV [37], resulting in the present energy window for the allowed iso-ex decay of $Q_{\beta,m}^* = -0.12(131)$ keV. Interestingly, hints of the 5_2^+ state being populated in the β^- -decay of $^{110}\text{Ag}^m$ have already been observed. The 846 keV γ ray, which is the strongest transition de-exciting the 5_2^+ state [37] was de-

tected in two studies [38, 39]. In addition, a second transition de-exciting this level, the 1466 keV γ ray, was observed in one of these studies [38]. However, both of them remain unplaced in the β^- -decay of ^{110}Ag [33, 38, 39]. All these facts make $^{110}\text{Ag}^m$ a perfect candidate for a potential ultra-low- Q_β^* transition.

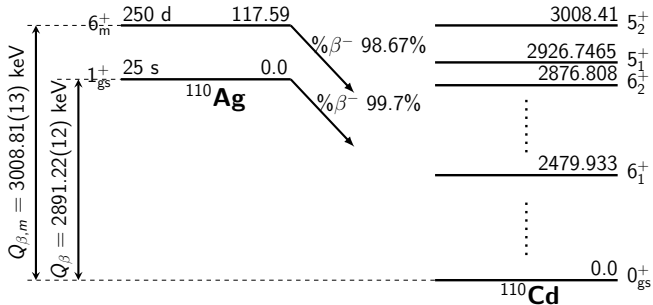


Figure 1. The β^- decay scheme of ^{110}Ag with the states in ^{110}Cd relevant for this work, based on Refs. [33, 37]. The Q_β values are from this work.

The masses of ^{109}Ag and ^{110}Ag isotopes are connected via a precise single-neutron separation energy value from the (n, γ) study ($S_n = 6809.19(11)$ keV [40]) while the $^{110}\text{Ag}^m$ and $^{110}\text{Cd}(5_2^+)$ excitation energies are known from γ -ray spectroscopy studies [33]. As a result, $Q_{\beta,m}^*$ can be expressed as a function of masses of two stable isotopes, ^{109}Ag and ^{110}Cd , and precise spectroscopic observables. Considering that the quadratically-added uncertainties of S_n , E_m and E_x are equal to 127 eV, the ≈ 1.3 keV uncertainty of $Q_{\beta,m}^*$ [32, 36] can be reduced if the single-proton separation energy (S_p) of ^{110}Cd is known with a precision better than 100 eV. In order to accomplish it, the mass of ^{109}Ag was determined with ^{110}Cd as a reference by utilizing the JYFLTRAP double Penning trap mass spectrometer [41] at the Ion Guide Isotope Separator On-Line (IGISOL) facility at the University of Jyväskylä [42]. This measurement results in the most precise determination of the $Q_{\beta,m}^*$, which is presented in this letter. To evaluate the potential of this transition for neutrino mass detection, we incorporated the precise $Q_{\beta,m}^*$ value into nuclear shell-model calculations using the KSHELL code with the jj45pnb interaction, combined with advanced atomic calculations. Additionally, to check for possible mass-dependent systematic effects caused by the $m(^{110}\text{Cd}) - m(^{109}\text{Ag}) \approx 1$ u mass difference, two mass measurements of zirconium oxide molecules, $^{90}\text{Zr}^{16}\text{O}$ and $^{92}\text{Zr}^{16}\text{O}$ with $^{91}\text{Zr}^{16}\text{O}$ as a reference, were also conducted, see Supplemental Material [43]. These molecules are in the same mass region as ^{109}Ag with nuclear masses that are well characterized [32, 36, 44, 45].

To produce the ions used in the measurements, a sample of natural silver was placed in an electric discharge ion source located in the target area of the IGISOL [42],

while samples of natural cadmium and zirconium were placed in the offline discharge ion source station [46]. The extracted ions were accelerated by a 30 kV electrostatic potential. The ions were transported through a 55° dipole magnet capable of separating the isobars containing the desired ions, $^{109}\text{Ag}^+$, $^{110}\text{Cd}^+$ and $^{90-92}\text{Zr}^+$, from the ion beam and allowing them to enter the radio-frequency quadrupole cooler-buncher [47]. In addition to cooling and bunching the beam for more efficient injection into the JYFLTRAP, the ZrO^+ molecules were formed there. Subsequently, the bunches were injected into the helium-filled preparation trap of JYFLTRAP [41], where the mass-selective buffer-gas cooling technique [48] was applied to separate the ions of interest from possible isobaric contaminants. The ions of interest were then sent to the measurement trap of JYFLTRAP.

In the measurement trap, the phase-imaging ion-cyclotron-resonance (PI-ICR) technique [49–52] was used to measure the free space cyclotron frequency $\nu_c = qB/(2\pi m)$ of an ion species, where q and m are the charge and mass of the ion and B the magnetic field strength. By measuring the cyclotron frequencies of an ion of interest ($\nu_{c,ioi}$) and a reference ion ($\nu_{c,ref}$), we obtain the ratio of the mass of the ion of interest to the mass of the reference from the ratio r of their frequencies, as

$$r = \frac{\nu_{c,ref}}{\nu_{c,ioi}} = \frac{m_{ioi}}{m_{ref}}. \quad (1)$$

With the PI-ICR technique, ν_c is determined by projecting the ions in the trap onto a position-sensitive microchannel plate detector (2D-MCP). The cyclotron frequency is obtained using the angle between the centers of the spots formed on the detector relative to the center spot after magnetron (α_-) and reduced cyclotron (α_+) eigenmotion accumulation

$$\nu_c = \frac{(\alpha_+ - \alpha_-) + 2\pi n_c}{2\pi t_{acc}}. \quad (2)$$

where t_{acc} is the accumulation time and n_c the number of revolutions during t_{acc} at frequency ν_c . Two timing patterns were used to excite the ions' radial eigenmotions using radiofrequency electric fields in order to produce the spots. At the start of both patterns, a dipolar pulse with frequency ν_- was used to reduce the initial magnetron motion of the ions to bring them to the center of the trap. Then for the magnetron spot, the pattern continued with a dipolar radiofrequency pulse with frequency ν_+ exciting the reduced cyclotron motion. This was followed by a quadrupolar pulse with frequency ν_c converting the motion to magnetron motion. Finally, after waiting for an accumulation time t_{acc} , the ions were projected onto the 2D-MCP registering their final positions. For the reduced cyclotron spot, the order of the converting pulse and the accumulation time was reversed. The position of the center of the trap on the 2D-MCP was

determined by extracting the centered ions without further excitations. Typical position data obtained in this work are shown in Fig. 2a) and b).

For the mass determination of ^{109}Ag , a total of 157 frequency ratios between $^{109}\text{Ag}^+$ and the reference $^{110}\text{Cd}^+$ were measured over 40 hours using three different accumulation times, 813 ms, 1 s and 1.5 s, see Fig. 2c). Two different spot positions on the detector were used to account for distortion in the projected image, but no systematic shift in the measured ratio was observed. A final ratio r was obtained as a weighted average of all the measurements. Similarly for $^{92}\text{Zr}^{16}\text{O}^+$ mass determination, 98 ratios over 25 hours were measured using two different spot positions and two accumulation times of 813 ms and 1 s, while for $^{90}\text{Zr}^{16}\text{O}^+$, 20 ratios with $t_{\text{acc}} = 1$ s were collected over five hours, both against the $^{91}\text{Zr}^{16}\text{O}^+$ reference, see Supplemental Material [43].

To reduce the effect of residual magnetron and cyclotron motion on the ions' position, the start of the conversion pulse was scanned over the cyclotron period ($\sim 1 \mu\text{s}$) and the extraction from the measurement trap over the period of the magnetron motion ($\sim 600 \mu\text{s}$). The effect of the temporal magnetic field fluctuation was minimized by alternating the measurements of the ion of interest and the reference ion every seven minutes and linearly interpolating the frequency ν_c of the reference at the time of the ion of interest measurement. The temporal fluctuation of the JYFLTRAP magnetic field has been measured to be $\delta B/(B\delta t) = 2.01 \times 10^{-12} \text{ min}^{-1}$ [52]. By performing count-rate class analysis [52–54] using bunches with up to five detected ions, the effect of ion-ion interactions was determined to be negligible.

The single-nucleon separation energy S_x can be determined from the frequency ratio r measured between two neighboring species:

$$S_x = [-|r-1| \times (m_{\text{ref}} - m_e) + m_x] c^2 + \frac{1-r}{|1-r|} (r B_{\text{ref}} - B_{\text{ioi}}), \quad (3)$$

where m_{ref} and m_e are the atomic mass of the reference species and the mass of an electron, respectively, while B_{ref} and B_{ioi} are the first ionization energies of the reference ion and the ion of interest, respectively, taken from Ref. [55]. For a single-neutron separation energy, m_x is the atomic mass of a neutron and for a single-proton separation energy m_x represents the mass of a hydrogen atom.

The measured frequency ratios and corresponding single-particle separation energies are presented in Table I. The ^{92}Zr single-neutron separation energy perfectly agrees with the Atomic Mass Evaluation 2020 (AME20) which is based on the (n, γ) study from Ref. [56]. At the same time, the $S_n(^{91}\text{Zr})$ value differs by 0.38(19) keV from AME20. However, it agrees with a value from the (n, γ) measurement [44] evaluated at ENSDF [45]. Considering that between the ion of interest and the reference

Table I. The frequency ratios r determined in this work with respect to the reference ions (Ref.) and the corresponding single-nucleon separation energies S_x (proton for ^{110}Cd , neutron for $^{91,92}\text{Zr}$) compared to the literature values $S_{x,\text{lit.}}$ from Refs. [36, 45, 56].

Nuclide	Ref.	$r = \nu_{c,\text{ref}}/\nu_c$	S_x (keV)	$S_{x,\text{lit.}}$ (keV)
^{109}Ag	^{110}Cd	0.99091693576(44)	8918.07(5)	8917.5(13)
$^{92}\text{Zr}^{16}\text{O}$	$^{91}\text{Zr}^{16}\text{O}$	1.00934887819(52)	8634.74(5)	8634.75(4)
$^{90}\text{Zr}^{16}\text{O}$	$^{91}\text{Zr}^{16}\text{O}$	0.9906366606(12)	7194.75(12)	7194.36(15) ^a
				7194.9(4) ^b

^a From AME20 [36].

^b From the ENSDF evaluation [45] based on the (n, γ) study from Ref. [44].

Table II. A comparison of Q_β values between different states in ^{110}Ag and ^{110}Cd from AME20 [36] and this work. The $^{110}\text{Ag}(6_m^+)$ and $^{110}\text{Cd}(5_2^+)$ excitation energies are taken from Refs. [32, 37].

Transition	AME20	This work
$1_{\text{gs}}^+ \rightarrow 0_{\text{gs}}^+$	2890.7(13) keV	2891.22(12) keV
$6_m^+ \rightarrow 0_{\text{gs}}^+$	3008.3(13) keV	3008.81(13) keV
$6_m^+ \rightarrow 5_2^+$	-0.12(131) keV	405(135) eV

ion there was only one mass unit of difference, the same as between ^{109}Ag and ^{110}Cd , and that the ZrO molecules are in the same mass region, no additional mass-dependent uncertainties are added to the ^{109}Ag frequency ratio.

The updated proton separation energy, $S_p(^{110}\text{Cd}) = 8918.07(5)$ keV, and the mass excess of ^{109}Ag (ME = $-88718.8(4)$ keV) are consistent with the values reported in AME20 ($S_{p,\text{lit.}}(^{110}\text{Cd}) = 8917.5(13)$ keV, ME_{lit.} = $-88719.4(13)$ keV [36]). These updated values are 26 and three times more precise, respectively, with the uncertainty in the latter being dominated by the uncertainty in the mass of ^{110}Cd . These results allows for reevaluation of the $Q_{\beta,m}$ value:

$$\begin{aligned} Q_{\beta,m} &= [m(^{110}\text{Ag}^m) - m(^{110}\text{Cd})] c^2 \\ &= [(r-1) \times (m(^{110}\text{Cd}) - m_e) + m_n] c^2 \\ &\quad + E_m - S_n + (r B_{\text{Cd}} - B_{\text{Ag}}), \end{aligned} \quad (4)$$

where $r = 0.99091693576(44)$ is the frequency ratio between $^{110}\text{Cd}^+$ and $^{109}\text{Ag}^+$ from this work, $m(^{110}\text{Cd}) = 109903007.5(4)$ μu is the atomic mass of ^{110}Cd [36], m_e and m_n are the masses of an electron and a neutron, respectively, $E_m = 117.59(5)$ keV [32] and $S_n = 6809.19(11)$ keV [40] are the $^{110}\text{Ag}^m$ excitation energy and the ^{110}Ag single-neutron separation energy, respectively, while $B_{\text{Cd}} = 8.993820(16)$ eV and $B_{\text{Ag}} = 7.576234(25)$ eV are the first ionization energies of Cd and Ag, respectively [55].

All the β -decay energies extracted in this work agree with AME20 [36] but they are an order of magnitude more precise, see Table II. The updated $Q_{\beta,m}^*$ value con-

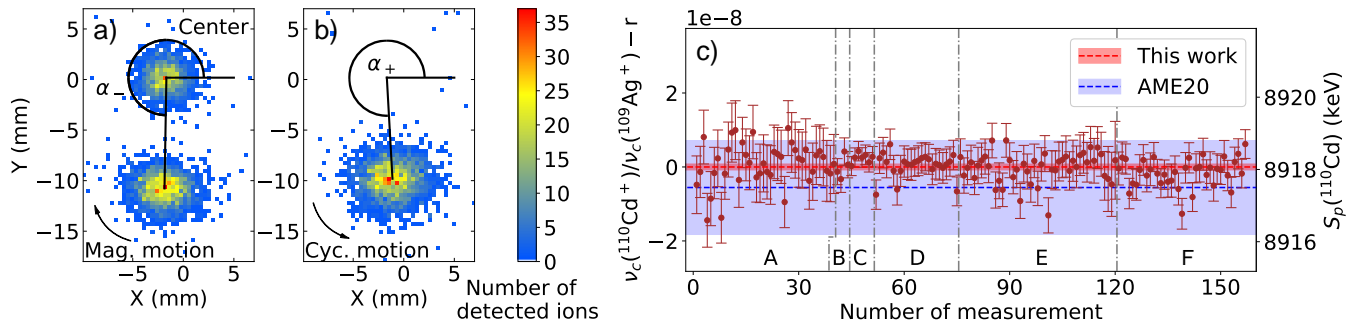


Figure 2. A PI-ICR measurement of a) magnetron and center spots and b) a cyclotron spot of $^{109}\text{Ag}^+$ ions collected on the 2D-MCP detector after 2.5 hours with $t_{\text{acc}} = 1$ s. c) Measured frequency ratios $\nu_c(^{110}\text{Cd}^+)/\nu_c(^{109}\text{Ag}^+)$ with the gray dotted lines indicating breaks in the measurement and the accumulation time change (A: $t_{\text{acc}} = 1$ s, B: $t_{\text{acc}} = 1$ s, C: $t_{\text{acc}} = 1.5$ s, D: $t_{\text{acc}} = 1$ s, E: $t_{\text{acc}} = 813$ ms and F: $t_{\text{acc}} = 1$ s). For the dataset E, the magnetron and reduced cyclotron spots were collected at $\alpha_- \approx \alpha_+ \approx 0^\circ$ while for other datasets $\alpha_- \approx \alpha_+ \approx 270^\circ$. The average frequency ratio $r = 0.990\,916\,935\,76(44)$ and the corresponding S_p value for ^{110}Cd are indicated with the red band while the AME20 value is plotted in blue.

firms that the transition is energetically allowed at a confidence level ($Q/\delta Q$) of 3σ , with $Q_{\beta,m}^* = 405(135)$ eV. It is the lowest observed Q_β^* value for an allowed transition and the second-lowest overall after the second-forbidden unique decay of ^{115}In to the first excited state in ^{115}Sn [31].

To estimate the partial half-lives for the decays of ^{110}Ag to the excited states in ^{110}Cd , we utilized the KSHELL code [57] within the Nuclear Shell Model (NSM) framework, employing the *jj45pn*b interaction [58], a two-nucleon potential based on a perturbative G-matrix approach. The model space includes the proton orbitals $0f_{5/2}$, $1p_{3/2}$, $1p_{1/2}$, and $1g_{9/2}$ with single-particle energies of -14.938 , -13.437 , -12.044 , and -8.905 MeV, respectively. For neutrons, the model space comprises the $0g_{7/2}$, $1d_{5/2}$, $1d_{3/2}$, $2s_{1/2}$, and $0h_{11/2}$ orbitals, with corresponding single-particle energies of 6.230 , 2.442 , 2.945 , 2.674 , and 4.380 MeV, as specified in the *jj45pn*b interaction. The computations were performed without truncation of the model space. We note that for the nuclear mass region around $A = 110$, only variants of the *jj45pn*b Hamiltonian are available in the libraries of the shell-model codes KSHELL and NuShellX@MSU [59]. All these variants produce similar results so that we consider here the results obtained by using the *jj45pn*b Hamiltonian as representative of all these Hamiltonians.

To validate the applied interaction, we computed the excitation energies, magnetic dipole and electric quadrupole moments for both ^{110}Ag and ^{110}Cd , and compared them with evaluated data, see Supplemental Material [43]. In computations of the electromagnetic moments, we have used standard effective charges $e_{\text{eff}}^p = 1.5e$ for protons and $e_{\text{eff}}^n = 0.5e$ for neutrons, and the bare g-factors $g_l(p) = 1$, $g_l(n) = 0$, $g_s(p) = 5.585$, and $g_s(n) = -3.826$. This choice leads to a reasonable agreement between the computed and measured electromagnetic moments, indicating that the wave functions of the

involved nuclear states are fairly reliable. The computed excitation energies of the 6_m^+ and 5_2^+ states, involved in the ultra-low- Q_β transition, correspond rather well to their experimental counterparts, thus speaking for their reliability in the half-life and branching estimations.

The major known allowed β -decay transitions from ^{110}Ag to ^{110}Cd as well as the transition of interest were computed and compared with experimental results, see Table III. These calculations included screening, radiative, and atomic exchange corrections, originally derived for allowed β decays and shown to have a stronger contribution at low electron energies [60]. Additionally, the effective weak axial coupling (g_A^{eff}) was varied between 0.5 and 0.8 as suggested in Ref. [61] for this mass region.

Since the phase-space factor is extremely sensitive to the decay energy, for the $6_m^+ \rightarrow 5_2^+$ transition the expected half-lives for the different g_A^{eff} values and for the $Q_{\beta,m}^*$ energies ranging from 225 to 600 eV are plotted, see Fig. 3. The experimental 1σ uncertainties found in this work are indicated by a gray shaded region. The partial half-life $t_{1/2}$ ranges from 3.70×10^6 y for the upper $Q_{\beta,m}^*$ limit (540 eV) with $g_A^{\text{eff}} = 0.80$ up to 7.47×10^7 y for the lower $Q_{\beta,m}^*$ limit (270 eV) with $g_A^{\text{eff}} = 0.5$. For any given g_A^{eff} curve, we mostly observe an order of magnitude difference in $t_{1/2}$ whilst considering the gray shaded area. The partial half-lives for two g_A^{eff} values, 0.5 and 0.8, were also computed without incorporating the atomic exchange corrections [60] to assess its impact. As can be seen in Fig. 3, the $t_{1/2}$ values increase by a factor ≈ 1.9 , and they range between 6.88×10^6 and 1.41×10^8 years. This result highlights the importance of this correction and emphasizes the importance of high-precision measurements of the ultra-low Q_β^* for the half-life determination. The observed discrepancies between theoretical predictions and experimental half-lives can be linked to limitations of the Nuclear Shell Model. These include the exclusion of orbitals outside the defined model space,

Table III. Comparison of experimental (column 2) and computed (columns 3-6) partial half-lives $t_{1/2}$ for allowed decays of ^{110}Ag to ^{110}Cd calculated with different values of the effective weak-axial coupling (g_A^{eff}). The NSM-computed Gamow-Teller matrix element (M_{GT}) and the experimental decay energies (Q_β^*) utilized in the computations are also presented. Experimental data was gathered from Refs. [33, 37] and this work.

Transition	Exp.	$t_{1/2}$					M_{GT}	Q_β^* (keV)
		0.5	0.6	0.7	0.8	Units		
$6_m^+ \rightarrow 6_1^+$	$808.51^{+8.06}_{-7.90}$	561.61	390.007	286.536	219.379	d	0.0117	528.88(13)
$6_m^+ \rightarrow 5_1^+$	$369.02^{+9.81}_{-4.24}$	117.627	81.6857	60.0139	45.9482	d	-0.4742	82.07(13)
$6_m^+ \rightarrow 5_2^+$	— ^a	22.309	15.492	11.382	8.714	My	0.1542	0.405(135)
$1_{\text{gs}}^+ \rightarrow 0_{\text{gs}}^+$	$25.88^{+0.20}_{-0.20}$	21.85	15.18	11.15	8.54	s	0.7271	2891.22(12)

^a This transition has not been observed experimentally yet.

the neglect of nuclear deformation effects, and the lack of fine-tuning of interaction parameters for this isotope. While addressing these issues would require significant effort, the results still serve as a valuable benchmark for evaluating the current computational framework.

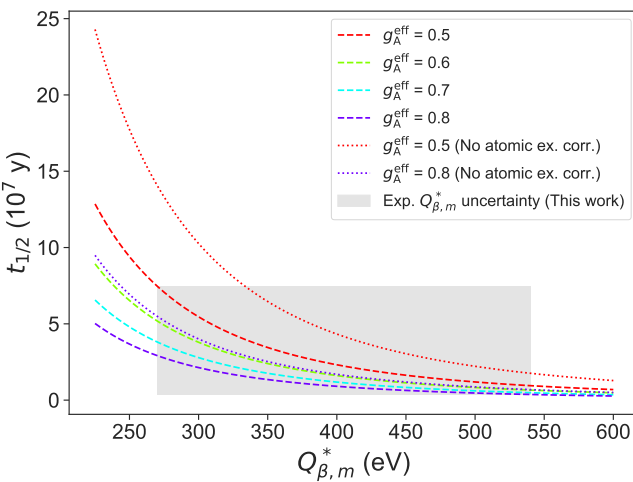


Figure 3. Theoretical estimates of the partial half-life $t_{1/2}$ of the allowed $^{110}\text{Ag}(6_m^+) \rightarrow ^{110}\text{Cd}(5_2^+)$ transition with a $Q_{\beta,m}^*$ value of 405(135) eV for different effective weak-axial coupling values (g_A^{eff}). The gray shaded area represents the 1σ uncertainty of the $Q_{\beta,m}^*$ value from this work. The dotted lines represent the computations without the atomic exchange correction.

The theoretical half-lives for the strongest β -decay branches are best reproduced when $g_A^{\text{eff}} = 0.5$, as shown in Table III. Therefore, this value was employed for the calculations concerning the main transition of interest. This choice is motivated entirely by its better overall agreement with experimental results, although it reflects a broader overreach of the nuclear shell model, suggesting that the model might not fully capture the quenching effects observed in experimental data. To estimate the influence of the energy window, the experimental $Q_{\beta,m}^*$ value was varied by 1σ . The resulting partial half-life is $2.23^{+5.24}_{-1.28} \times 10^7$ years, which corresponds to a branching

ratio of $3.07^{+4.16}_{-2.15} \times 10^{-8}$ for the $^{110}\text{Ag}(6_m^+) \rightarrow ^{110}\text{Cd}(5_2^+)$ decay.

In summary, we have measured with high precision the single-proton separation energy of ^{110}Cd , $S_p = 8918.07(5)$ keV, resulting in the improved mass-excess value of ^{109}Ag , ME = $-88718.8(4)$ keV. By combining our results with the well known single-neutron separation energy and the isomer excitation energy of ^{110}Ag , we demonstrated that the $^{110}\text{Ag}(6_m^+) \rightarrow ^{110}\text{Cd}^*(5_2^+)$ β -decay transition has the ultra-low Q_β^* value of 405(135) eV. This is the lowest Q_β^* for any allowed transition measured to date and the first low Q_β^* case measured for a β -decaying isomer. The nuclear shell model combined with the atomic calculations predicted the partial half-life for this transition to be $2.23^{+5.24}_{-1.28} \times 10^7$ years which translates to the branching ratio of $3.07^{+4.16}_{-2.15} \times 10^{-8}$. It should be noted that if the 846 keV and 1466 keV γ rays observed in the decay studies of ^{110}Ag originate from the de-excitation of the 5_2^+ state in ^{110}Cd , the partial decay half-life to this state would be in the $10^3 - 10^4$ years range, which is orders of magnitude shorter than indicated by calculations. All in all, our work indicates that $^{110}\text{Ag}^m$ might be a good candidate for the future antineutrino mass measurement experiments, although a new decay study of $^{110}\text{Ag}^m$ is required to confirm the production of the 5_2^+ state in ^{110}Cd . Our work also demonstrates that the future search of low- Q_β^* transitions should not be limited to the β -decaying ground states, with the isomers in $^{101,102}\text{Rh}$, ^{106}Ag , ^{120}Sb , ^{121}Te , ^{184}Re and ^{194}Ir being the most promising cases to find such transitions.

This project has received funding from the European Union's Horizon 2020 research and innovation programme under grant agreement No. 771036 (ERC CoG MAIDEN), from the European Union's Horizon Europe Research and Innovation Programme under Grant Agreement No. 101057511 (EURO-LABS) and the Research Council of Finland projects No. 295207, 306980, 327629, 354589 and 354968. J.R. acknowledges the financial support from the Vilho, Yrjö and Kalle Väisälä Foundation.

* jouni.k.a.ruotsalainen@jyu.fi
 † marek.m.stryjczyk@jyu.fi
 ‡ madeoliv@jyu.fi
 § jouni.t.suhonen@jyu.fi

- [1] The KATRIN collaboration, M. Aker, K. Altenmüller, J.F. Amsbaugh, M. Arenz, M. Babutzka, J. Bast, S. Bauer, H. Bechtler, M. Beck, A. Beglarian, J. Behrens, B. Bender, R. Berendes, A. Berlev, U. Besserer, C. Bettin, B. Bieringer, K. Blaum, F. Block, S. Bobien, M. Böttcher, J. Bohn, K. Bokeloh, H. Bolz, B. Bornschein, L. Bornschein, H. Bouquet, N.M. Boyd, T. Brunst, T.H. Burritt, T.S. Caldwell, Z. Chaoui, S. Chilingaryan, W. Choi, T.J. Corona, G.A. Cox, K. Debowski, M. Deffert, M. Descher, D. Díaz Barrero, P.J. Doe, O. Dragoun, G. Drexlin, J.A. Dunmore, S. Dyba, F. Edzards, F. Eichelhardt, K. Eitel, E. Ellinger, R. Engel, S. Enomoto, M. Erhard, D. Eversheim, M. Fedkevych, A. Felden, S. Fischer, J.A. Formaggio, F.M. Fränkle, G.B. Franklin, H. Frenzel, F. Friedel, A. Fulst, K. Gauda, R. Gehring, W. Gil, F. Glück, S. Görhardt, J. Grimm, R. Grössle, S. Groh, S. Grohmann, R. Gumbshemer, M. Hackenjos, D. Häfler, V. Hannen, F. Harms, G.C. Harper, J. Hartmann, N. Haußmann, F. Heizmann, K. Helbing, M. Held, S. Hickford, D. Hilk, B. Hillen, R. Hiller, D. Hillesheimer, D. Hinz, T. Höhn, M. Hötzl, S. Holzmann, S. Horn, T. Houdy, M.A. Howe, A. Huber, T. James, A. Jansen, M. Kaiser, C. Karl, O. Kazachenko, J. Kellerer, L. Kippenbrock, M. Kleesiek, M. Kleifges, J. Kleinfeller, M. Klein, C. Köhler, L. Köllenberger, A. Kopmann, M. Korzeczek, A. Kosmider, A. Kovalík, B. Krasch, H. Krause, M. Kraus, L. Kuckert, A. Kumb, N. Kunka, T. Lasserre, L. La Cascio, O. Lebeda, M.L. Leber, B. Lehnert, B. Leiber, J. Letnev, R.J. Lewis, T.L. Le, S. Lichter, A. Lokhov, J.M. Lopez Poyato, M. Machatschek, E. Malcherek, M. Mark, A. Marsteller, E.L. Martin, K. Mehret, M. Meloni, C. Melzer, A. Menshikov, S. Mertens, L.I. Minter (née Bodine), B. Montreal, J. Mostafa, K. Müller, A.W. Myers, U. Naumann, H. Neumann, S. Niemes, P. Oelpmann, A. Off, H.-W. Rodejohann, A. Osipowicz, B. Ostrik, D.S. Parno, D.A. Peterson, P. Plischke, A.W.P. Poon, M. Prall, F. Priester, P.C.-O. Ranitzsch, J. Reich, P. Renschler, O. Rest, R. Rinderspacher, R.G.H. Robertson, W. Rodejohann, C. Rodenbeck, M. Röllig, C. Rötttele, P. Rohr, S. Rupp, M. Ryšavý, R. Sack, A. Saenz, M. Sagawe, P. Schäfer, A. Schaller (née Pollithy), L. Schimpf, K. Schlösser, M. Schlösser, L. Schlüter, S. Schneidewind, H. Schön, K. Schönung, M. Schrank, B. Schulz, J. Schwarz, M. Šefčík, H. Seitz-Moskaliuk, W. Seller, V. Sibille, D. Siegmann, M. Slezák, F. Spanier, M. Steidl, M. Sturm, M. Sun, D. Tcherniakhovski, H.H. Telle, L.A. Thorne, T. Thümmler, N. Titov, I. Tkachev, N. Trost, K. Urban, K. Valerius, B.A. VanDevender, T.D. Van Wechel, D. Vénos, A. Verbeek, R. Vianden, A.P. Vizcaya Hernández, K. Vogt, B.L. Wall, N. Wandkowsky, M. Weber, H. Weingardt, C. Weinheimer, C. Weiss, S. Welte, J. Wendel, K.J. Wierman, J.F. Wilkerson, J. Wolf, S. Wüstling, W. Xu, Y.-R. Yen, M. Zacher, S. Zadorogny, M. Zboril, and G. Zeller, The design, construction, and commissioning of the KATRIN experiment, *Journal of Instrumentation* **16** (08), T08015.
- [2] The KATRIN Collaboration, M. Aker, A. Beglarian, J. Behrens, A. Berlev, U. Besserer, B. Bieringer, F. Block, S. Bobien, M. Böttcher, B. Bornschein, L. Bornschein, T. Brunst, T. S. Caldwell, R. M. D. Carney, L. La Cascio, S. Chilingaryan, W. Choi, K. Debowski, M. Deffert, M. Descher, D. Díaz Barrero, P. J. Doe, O. Dragoun, G. Drexlin, K. Eitel, E. Ellinger, R. Engel, S. Enomoto, A. Felden, J. A. Formaggio, F. M. Fränkle, G. B. Franklin, F. Friedel, A. Fulst, K. Gauda, W. Gil, F. Glück, R. Grössle, R. Gumsheimer, V. Gupta, T. Höhn, V. Hannen, N. Haußmann, K. Helbing, S. Hickford, R. Hiller, D. Hillesheimer, D. Hinz, T. Houdy, A. Huber, A. Jansen, C. Karl, F. Kellerer, J. Kellerer, M. Kleifges, M. Klein, C. Köhler, L. Köllenberger, A. Kopmann, M. Korzeczek, A. Kovalík, B. Krasch, H. Krause, N. Kunka, T. Lasserre, T. L. Le, O. Lebeda, B. Lehnert, A. Lokhov, M. Machatschek, E. Malcherek, M. Mark, A. Marsteller, E. L. Martin, C. Melzer, A. Menshikov, S. Mertens, J. Mostafa, K. Müller, H. Neumann, S. Niemes, P. Oelpmann, D. S. Parno, A. W. P. Poon, J. M. L. Poyato, F. Priester, S. Ramachandran, R. G. H. Robertson, W. Rodejohann, M. Röllig, C. Rötttele, C. Rodenbeck, M. Ryšavý, R. Sack, A. Saenz, P. Schäfer, A. Schaller née Pollithy, L. Schimpf, K. Schlösser, M. Schlösser, L. Schlüter, S. Schneidewind, M. Schrank, B. Schulz, A. Schwemmer, M. Šefčík, V. Sibille, D. Siegmann, M. Slezák, F. Spanier, M. Steidl, M. Sturm, M. Sun, D. Tcherniakhovski, H. H. Telle, L. A. Thorne, T. Thümmler, N. Titov, I. Tkachev, K. Urban, K. Valerius, D. Vénos, A. P. Vizcaya Hernández, C. Weinheimer, S. Welte, J. Wendel, J. F. Wilkerson, J. Wolf, S. Wüstling, J. Wydra, W. Xu, Y.-R. Yen, S. Zadorogny, and G. Zeller, Direct neutrino-mass measurement with sub-electronvolt sensitivity, *Nature Physics* **18**, 160 (2022).
- [3] A. Nucciotti, The MARE Project, *Journal of Low Temperature Physics* **151**, 597 (2008).
- [4] E. Ferri, D. Bagliani, M. Biasotti, G. Ceruti, D. Corsini, M. Faverzani, F. Gatti, A. Giachero, C. Gotti, C. Kilbourne, A. Kling, M. Maino, P. Manfrinetti, A. Nucciotti, G. Pessina, G. Pizzigoni, M. Ribeiro Gomes, and M. Sisti, The Status of the MARE Experiment with ^{187}Re and ^{163}Ho Isotopes, *Physics Procedia* **61**, 227 (2015).
- [5] L. Gastaldo, K. Blaum, K. Chrysalidis, T. Day Goodacre, A. Domula, M. Door, H. Dorrer, C. E. Düllmann, K. Eberhardt, S. Eliseev, C. Enss, A. Faessler, P. Filianin, A. Fleischmann, D. Fonnesu, L. Gamer, R. Haas, C. Hassel, D. Hengstler, J. Jochum, K. Johnston, U. Kebeschull, S. Kempf, T. Kieck, U. Köster, S. Lahiri, M. Maiti, F. Mantegazzini, B. Marsh, P. Neroutsos, Y. N. Novikov, P. C. O. Ranitzsch, S. Rothe, A. Rischka, A. Saenz, O. Sander, F. Schneider, S. Scholl, R. X. Schüssler, C. Schweiger, F. Simkovic, T. Stora, Z. Szűcs, A. Türler, M. Veinhard, M. Weber, M. Wegner, K. Wendt, and K. Zuber, The electron capture in ^{163}Ho experiment – ECHO, *The European Physical Journal Special Topics* **226**, 1623 (2017).
- [6] C. Velte, F. Ahrens, A. Barth, K. Blaum, M. Braß, M. Door, H. Dorrer, C. E. Düllmann, S. Eliseev, C. Enss, P. Filianin, A. Fleischmann, L. Gastaldo, A. Goeggemann, T. D. Goodacre, M. W. Haverkort, D. Hengstler, J. Jochum, K. Johnston, M. Keller, S. Kempf, T. Kieck, C. M. König, U. Köster, K. Kromer, F. Mantegazzini, B. Marsh, Y. N. Novikov, F. Pique-

- mal, C. Riccio, D. Richter, A. Rischka, S. Rothe, R. X. Schüssler, C. Schweiger, T. Stora, M. Wegner, K. Wendt, M. Zampaolo, and K. Zuber, High-resolution and low-background ^{163}Ho spectrum: interpretation of the resonance tails, *The European Physical Journal C* **79**, 1026 (2019).
- [7] M. Faverzani, B. Alpert, D. Backer, D. Bennet, M. Biasotti, C. Brofferio, V. Ceriale, G. Ceruti, D. Corsini, P. K. Day, M. De Gerone, R. Dressler, E. Ferri, J. Fowler, E. Fumagalli, J. Gard, F. Gatti, A. Giachero, J. Hays-Wehle, S. Heinitz, G. Hilton, U. Köster, M. Lusignoli, M. Maino, J. Mates, S. Nisi, R. Nizzolo, A. Nucciotti, A. Orlando, L. Parodi, G. Pessina, G. Pizzigoni, A. Puiu, S. Ragazzi, C. Reintsema, M. Ribeiro-Gomez, D. Schmidt, D. Schuman, F. Siccardi, M. Sisti, D. Swetz, F. Terranova, J. Ullom, and L. Vale, The HOLMES Experiment, *Journal of Low Temperature Physics* **184**, 922 (2016).
- [8] M. De Gerone, B. Alpert, M. Balata, D. T. Becker, D. A. Bennett, A. Bevilacqua, M. Borghesi, G. Ceruti, G. D. B. De Galember, R. Dressler, M. Faverzani, M. Fedkevych, E. Ferri, J. W. Fowler, G. Gallucci, J. D. Gard, F. Gatti, A. Giachero, G. C. Hilton, U. Köster, M. Lusignoli, P. Manfrinetti, J. A. B. Mates, E. Maugeri, S. Nisi, A. Nucciotti, L. Parodi, G. Pessina, S. Ragazzi, C. D. Reintsema, D. R. Schmidt, D. Schumann, F. Siccardi, D. S. Swetz, J. N. Ullom, and L. R. Vale, Status of the HOLMES Experiment, *Journal of Low Temperature Physics* **209**, 980 (2022).
- [9] W. C. Pettus and on behalf of the Project 8 Collaboration, Overview of Project 8 and Progress Towards Tritium Operation, *Journal of Physics: Conference Series* **1342**, 012040 (2020).
- [10] M. Medina Restrepo and E. G. Myers, Mass Difference of Tritium and Helium-3, *Phys. Rev. Lett.* **131**, 243002 (2023).
- [11] C. Schweiger, M. Braß, V. Debierre, M. Door, H. Dorrer, C. E. Düllmann, C. Enss, P. Filianin, L. Gastaldo, Z. Harman, M. W. Haverkort, J. Herkenhoff, P. Indelicato, C. H. Keitel, K. Kromer, D. Lange, Y. N. Novikov, D. Renisch, A. Rischka, R. X. Schüssler, S. Eliseev, and K. Blaum, Penning-trap measurement of the Q value of electron capture in ^{163}Ho for the determination of the electron neutrino mass, *Nature Physics* **20**, 921 (2024).
- [12] P. Filianin, C. Lyu, M. Door, K. Blaum, W. J. Huang, M. Haverkort, P. Indelicato, C. H. Keitel, K. Kromer, D. Lange, Y. N. Novikov, A. Rischka, R. X. Schüssler, C. Schweiger, S. Sturm, S. Ulmer, Z. Harman, and S. Eliseev, Direct Q -Value Determination of the β^- Decay of ^{187}Re , *Phys. Rev. Lett.* **127**, 072502 (2021).
- [13] J. Kopp and A. Merle, Ultralow Q values for neutrino mass measurements, *Phys. Rev. C* **81**, 045501 (2010).
- [14] J. S. E. Wieslander, J. Suhonen, T. Eronen, M. Hult, V.-V. Elomaa, A. Jokinen, G. Marissens, M. Misiaszek, M. T. Mustonen, S. Rahaman, C. Weber, and J. Äystö, Smallest Known Q Value of Any Nuclear Decay: The Rare β^- Decay of $^{115}\text{In}(9/2^+) \rightarrow ^{115}\text{Sn}(3/2^+)$, *Phys. Rev. Lett.* **103**, 122501 (2009).
- [15] E. Andreotti, M. Hult, R. González de Orduña, G. Marissens, J. S. E. Wieslander, and M. Misiaszek, Half-life of the β decay $^{115}\text{In}(9/2^+) \rightarrow ^{115}\text{Sn}(3/2^+)$, *Phys. Rev. C* **84**, 044605 (2011).
- [16] B. J. Mount, M. Redshaw, and E. G. Myers, Q Value of $^{115}\text{In} \rightarrow ^{115}\text{Sn}(3/2^+)$: The Lowest Known Energy β Decay, *Phys. Rev. Lett.* **103**, 122502 (2009).
- [17] A. de Roubin, J. Kostensalo, T. Eronen, L. Canete, R. P. de Groote, A. Jokinen, A. Kankainen, D. A. Nesterenko, I. D. Moore, S. Rinta-Antila, J. Suhonen, and M. Vilén, High-Precision Q -Value Measurement Confirms the Potential of ^{135}Cs for Absolute Antineutrino Mass Scale Determination, *Phys. Rev. Lett.* **124**, 222503 (2020).
- [18] T. Eronen, Z. Ge, A. de Roubin, M. Ramalho, J. Kostensalo, J. Kotila, O. Beliuskina, C. Delafosse, S. Geldhof, W. Gins, M. Hukkanen, A. Jokinen, A. Kankainen, I.D. Moore, D.A. Nesterenko, M. Stryjczyk, and J. Suhonen, High-precision measurement of a low Q value for allowed β^- -decay of ^{131}I related to neutrino mass determination, *Physics Letters B* **830**, 137135 (2022).
- [19] Z. Ge, T. Eronen, K. S. Tyrin, J. Kotila, J. Kostensalo, D. A. Nesterenko, O. Beliuskina, R. de Groote, A. de Roubin, S. Geldhof, W. Gins, M. Hukkanen, A. Jokinen, A. Kankainen, A. Koszorús, M. I. Krivoruchenko, S. Kujanpää, I. D. Moore, A. Raggio, S. Rinta-Antila, J. Suhonen, V. Virtanen, A. P. Weaver, and A. Zadvornaya, ^{159}Dy Electron-Capture: A New Candidate for Neutrino Mass Determination, *Phys. Rev. Lett.* **127**, 272301 (2021).
- [20] R. Sandler, G. Bollen, N. D. Gamage, A. Hamaker, C. Izzo, D. Puentes, M. Redshaw, R. Ringle, and I. Yandow, Investigation of the potential ultralow Q -value β -decay candidates ^{89}Sr and ^{139}Ba using Penning trap mass spectrometry, *Phys. Rev. C* **100**, 024309 (2019).
- [21] J. Karthein, D. Atanasov, K. Blaum, S. Eliseev, P. Filianin, D. Lunney, V. Manea, M. Mougeot, D. Neidherr, Y. Novikov, L. Schweikhard, A. Welker, F. Wienholtz, and K. Zuber, Direct decay-energy measurement as a route to the neutrino mass, *Hyperfine Interactions* **240**, 61 (2019).
- [22] Z. Ge, T. Eronen, A. de Roubin, D. A. Nesterenko, M. Hukkanen, O. Beliuskina, R. de Groote, S. Geldhof, W. Gins, A. Kankainen, A. Koszorús, J. Kotila, J. Kostensalo, I. D. Moore, A. Raggio, S. Rinta-Antila, J. Suhonen, V. Virtanen, A. P. Weaver, A. Zadvornaya, and A. Jokinen, Direct measurement of the mass difference of $^{72}\text{As}-^{72}\text{Ge}$ rules out ^{72}As as a promising β -decay candidate to determine the neutrino mass, *Phys. Rev. C* **103**, 065502 (2021).
- [23] M. Ramalho, Z. Ge, T. Eronen, D. A. Nesterenko, J. Jaatinen, A. Jokinen, A. Kankainen, J. Kostensalo, J. Kotila, M. I. Krivoruchenko, J. Suhonen, K. S. Tyrin, and V. Virtanen, Observation of an ultralow- Q -value electron-capture channel decaying to ^{75}As via a high-precision mass measurement, *Phys. Rev. C* **106**, 015501 (2022).
- [24] Z. Ge, T. Eronen, A. de Roubin, K.S. Tyrin, L. Canete, S. Geldhof, A. Jokinen, A. Kankainen, J. Kostensalo, J. Kotila, M.I. Krivoruchenko, I.D. Moore, D.A. Nesterenko, J. Suhonen, and M. Vilén, High-precision electron-capture Q value measurement of ^{111}In for electron-neutrino mass determination, *Physics Letters B* **832**, 137226 (2022).
- [25] Z. Ge, T. Eronen, A. de Roubin, J. Kostensalo, J. Suhonen, D. A. Nesterenko, O. Beliuskina, R. de Groote, C. Delafosse, S. Geldhof, W. Gins, M. Hukkanen, A. Jokinen, A. Kankainen, J. Kotila, A. Koszorús, I. D. Moore, A. Raggio, S. Rinta-Antila, V. Virtanen, A. P. Weaver, and A. Zadvornaya, Direct determination of the atomic mass difference of the pairs $^{76}\text{As}-^{76}\text{Se}$ and $^{155}\text{Tb}-^{155}\text{Gd}$

- rules out ^{76}As and ^{155}Tb as possible candidates for electron (anti)neutrino mass measurements, *Phys. Rev. C* **106**, 015502 (2022).
- [26] N. D. Gamage, R. Sandler, F. Buchinger, J. A. Clark, D. Ray, R. Orford, W. S. Porter, M. Redshaw, G. Savard, K. S. Sharma, and A. A. Valverde, Precise Q -value measurements of $^{112,113}\text{Ag}$ and ^{115}Cd with the Canadian Penning trap for evaluation of potential ultralow Q -value β decays, *Phys. Rev. C* **106**, 045503 (2022).
- [27] M. Horana Gamage, R. Bhandari, G. Bollen, N. D. Gamage, A. Hamaker, D. Puentes, M. Redshaw, R. Ringle, S. Schwarz, C. S. Sumithrarachchi, and I. Yandow, Identification of a potential ultralow- Q -value electron-capture decay branch in ^{75}Se via a precise Penning trap measurement of the mass of ^{75}As , *Phys. Rev. C* **106**, 065503 (2022).
- [28] Z. Ge, T. Eronen, A. de Roubin, M. Ramalho, J. Kostensalo, J. Kotila, J. Suhonen, D. A. Nesterenko, A. Kankainen, P. Ascher, O. Beliuskina, M. Flayol, M. Gerbaux, S. Grévy, M. Hukkanen, A. Husson, A. Jaries, A. Jokinen, I. D. Moore, P. Pirinen, J. Romero, M. Stryjczyk, V. Virtanen, and A. Zadvornaya, β^- decay Q -value measurement of ^{136}Cs and its implications for neutrino studies, *Phys. Rev. C* **108**, 045502 (2023).
- [29] Z. Ge, T. Eronen, M. Ramalho, A. de Roubin, D. A. Nesterenko, A. Kankainen, O. Beliuskina, R. de Groote, S. Geldhof, W. Gins, M. Hukkanen, A. Jokinen, Á. Koszorús, J. Kotila, J. Kostensalo, I. D. Moore, P. Pirinen, A. Raggio, S. Rinta-Antila, V. A. Sevestrean, J. Suhonen, V. Virtanen, and A. Zadvornaya, Direct high-precision measurement of the mass difference of ^{77}As - ^{77}Se related to neutrino mass determination, *The European Physical Journal A* **60**, 104 (2024).
- [30] Z. Ge, T. Eronen, V. A. Sevestrean, O. Nițescu, S. Stoica, M. Ramalho, J. Suhonen, A. de Roubin, D. Nesterenko, A. Kankainen, P. Ascher, S. Ayet San Andres, O. Beliuskina, P. Delahaye, M. Flayol, M. Gerbaux, S. Grévy, M. Hukkanen, A. Jaries, A. Jokinen, A. Husson, D. Kahl, J. Kostensalo, J. Kotila, I. Moore, S. Nikas, M. Stryjczyk, and V. Virtanen, High-precision measurements of the atomic mass and electron-capture decay Q value of ^{95}Tc , *Physics Letters B* **859**, 139094 (2024).
- [31] D. K. Kebelbeck, R. Bhandari, N. D. Gamage, M. Horana Gamage, K. G. Leach, X. Mougeot, and M. Redshaw, Updated evaluation of potential ultralow Q -value β -decay candidates, *Phys. Rev. C* **107**, 015504 (2023).
- [32] F.G. Kondev, M. Wang, W.J. Huang, S. Naimi, and G. Audi, The NUBASE2020 evaluation of nuclear physics properties, *Chinese Physics C* **45**, 030001 (2021).
- [33] G. Gürdal and F.G. Kondev, Nuclear Data Sheets for $A = 110$, *Nuclear Data Sheets* **113**, 1315 (2012).
- [34] S. Nakamura, H. Wada, O. Shcherbakov, K. Furutaka, H. Harada, and T. Katoh, Measurement of the Thermal Neutron Capture Cross Section and the Resonance Integral of the $^{109}\text{Ag}(n, \gamma)^{110m}\text{Ag}$ Reaction, *Journal of Nuclear Science and Technology* **40**, 119 (2003).
- [35] E. K. Elmaghriby, E. Salem, Z. Yousef, and N. El-Anwar, Role of isomeric state formation on the measurement of thermal neutron cross section and resonance integral, *Physica Scripta* **94**, 015301 (2018).
- [36] Meng Wang, W.J. Huang, F.G. Kondev, G. Audi, and S. Naimi, The AME 2020 atomic mass evaluation (II). Tables, graphs and references, *Chinese Physics C* **45**, 030003 (2021).
- [37] B. Singh, Compiled (unevaluated) dataset from Refs. [62] and [63], compiled on 15 Jun 2020, from XUNDL database as of 01 Sep 2024. Version available at <https://www.nndc.bnl.gov/xundlarchivals/>.
- [38] G. Mallet, Measurement of the Radioactive Decay of $^{110}\text{Ag}^{m+g}$, *Journal of the Physical Society of Japan* **50**, 384 (1981).
- [39] L. Kiang, P. Teng, G. Kiang, W. Chang, and P. Tu, Study on the Level Structure of ^{110}Cd Populated by the Beta Decay of ^{110m}Ag , *Journal of the Physical Society of Japan* **62**, 888 (1993).
- [40] M. Bogdanovic, T.D. Mac Mahon, and H. Seyfarth, Low-Lying States in Doubly-Odd ^{108}Ag and ^{110}Ag , in *Annual Report / Kernforschungsanlage Jülich Institut für Kernphysik : 1980*, JUL-Spez-99,P76 (Kernforschungsanlage Jülich GmbH Zentralbibliothek, Verlag, 1981) p. 76.
- [41] T. Eronen, V. S. Kolhinen, V. V. Elomaa, D. Gorelov, U. Hager, J. Hakala, A. Jokinen, A. Kankainen, P. Karvonen, S. Kopecky, I. D. Moore, H. Penttilä, S. Rahaman, S. Rinta-Antila, J. Rissanen, A. Saastamoinen, J. Szerypo, C. Weber, and J. Äystö, JYFLTRAP: a Penning trap for precision mass spectroscopy and isobaric purification, *The European Physical Journal A* **48**, 46 (2012).
- [42] I.D. Moore, T. Eronen, D. Gorelov, J. Hakala, A. Jokinen, A. Kankainen, V.S. Kolhinen, J. Koponen, H. Penttilä, I. Pohjalainen, M. Reponen, J. Rissanen, A. Saastamoinen, S. Rinta-Antila, V. Sonnenschein, and J. Äystö, Towards commissioning the new IGISOL-4 facility, *Nuclear Instruments and Methods in Physics Research Section B: Beam Interactions with Materials and Atoms* **317**, 208 (2013).
- [43] See Supplemental Material at [URL will be inserted by publisher] for an additional Figure with the measured frequency ratios and Tables with the results of Nuclear Shell Model calculations compared with experimental data from Refs. [33, 37, 64–67].
- [44] M. A. Lone and G. A. Bartholomew, $^{90}\text{Zr}(n, \gamma)$ Studies with Thermal Neutrons, in *Neutron Capture Gamma-Ray Spectroscopy*, edited by R. E. Chrien and W. R. Kane (Springer US, Boston, MA, 1979) pp. 675–677.
- [45] C. M. Baglin, Nuclear Data Sheets for $A = 91$, *Nuclear Data Sheets* **114**, 1293 (2013).
- [46] M. Vilén, L. Canete, B. Cheal, A. Giatzoglou, R. de Groote, A. de Roubin, T. Eronen, S. Geldhof, A. Jokinen, A. Kankainen, I.D. Moore, D.A. Nesterenko, H. Penttilä, I. Pohjalainen, M. Reponen, and S. Rinta-Antila, A new off-line ion source facility at IGISOL, *Nuclear Instruments and Methods in Physics Research Section B: Beam Interactions with Materials and Atoms* **463**, 382 (2020).
- [47] A. Nieminen, J. Huikari, A. Jokinen, J. Äystö, P. Campbell, and E.C.A. Cochran, Beam cooler for low-energy radioactive ions, *Nuclear Instruments and Methods in Physics Research Section A: Accelerators, Spectrometers, Detectors and Associated Equipment* **469**, 244 (2001).
- [48] G. Savard, St. Becker, G. Bollen, H.-J. Kluge, R. Moore, T. Otto, L. Schweikhard, H. Stolzenberg, and U. Wiess, A new cooling technique for heavy ions in a Penning trap, *Physics Letters A* **158**, 247 (1991).
- [49] S. Eliseev, K. Blaum, M. Block, C. Droese, M. Goncharov, E. Minaya Ramirez, D. A. Nesterenko, Y. N. Novikov, and L. Schweikhard, Phase-Imaging Ion-Cyclotron-Resonance Measurements for Short-Lived Nuclides, *Phys. Rev. Lett.* **110**, 082501 (2013).

- [50] S. Eliseev, K. Blaum, M. Block, A. Dörr, C. Droese, T. Eronen, M. Goncharov, M. Höcker, J. Ketter, E. M. Ramirez, D. A. Nesterenko, Y. N. Novikov, and L. Schweikhard, A phase-imaging technique for cyclotron-frequency measurements, *Applied Physics B* **114**, 107 (2014).
- [51] D. A. Nesterenko, T. Eronen, A. Kankainen, L. Canete, A. Jokinen, I. D. Moore, H. Penttilä, S. Rinta-Antila, A. de Roubin, and M. Vilen, Phase-Imaging Ion-Cyclotron-Resonance technique at the JYFLTRAP double Penning trap mass spectrometer, *The European Physical Journal A* **54**, 154 (2018).
- [52] D. A. Nesterenko, T. Eronen, Z. Ge, A. Kankainen, and M. Vilen, Study of radial motion phase advance during motion excitations in a Penning trap and accuracy of JYFLTRAP mass spectrometer, *The European Physical Journal A* **57**, 302 (2021).
- [53] A. Kellerbauer, K. Blaum, G. Bollen, F. Herfurth, H.-J. Kluge, M. Kuckein, E. Sauvan, C. Scheidenberger, and L. Schweikhard, From direct to absolute mass measurements: A study of the accuracy of ISOLTRAP, *Eur. Phys. J. D* **22**, 53 (2003).
- [54] C. Roux, K. Blaum, M. Block, C. Droese, S. Eliseev, M. Goncharov, F. Herfurth, E. M. Ramirez, D. A. Nesterenko, Y. N. Novikov, and L. Schweikhard, Data analysis of Q-value measurements for double-electron capture with SHIPTRAP, *The European Physical Journal D* **67**, 146 (2013).
- [55] A. Kramida, Y. Ralchenko, J. Reader, and NIST ASD Team, *NIST Standard Reference Database 78, Version 5.10* (2022).
- [56] T. Rząca-Urban, W. Urban, M. Czerwiński, J. Wiśniewski, A. Blanc, H. Faust, M. Jentschel, P. Mutti, U. Köster, T. Soldner, G. de France, G. S. Simpson, and C. A. Ur, Low-spin excitations in ^{97}Zr , *Phys. Rev. C* **98**, 064315 (2018).
- [57] N. Shimizu, T. Mizusaki, Y. Utsuno, and Y. Tsunoda, Thick-restart block Lanczos method for large-scale shell-model calculations, *Computer Physics Communications* **244**, 372 (2019).
- [58] A. F. Lisetskiy, B. A. Brown, M. Horoi, and H. Grawe, New $T = 1$ effective interactions for the $f_{5/2} p_{3/2} p_{1/2} g_{9/2}$ model space: Implications for valence-mirror symmetry and seniority isomers, *Phys. Rev. C* **70**, 044314 (2004).
- [59] B. A. Brown and W. D. M. Rae, The Shell-Model Code NuShellX@MSU, *Nuclear Data Sheets* **120**, 115 (2014).
- [60] O. Nițescu, S. Stoica, and F. Šimkovic, Exchange correction for allowed β decay, *Phys. Rev. C* **107**, 025501 (2023).
- [61] H. Ejiri, J. Suhonen, and K. Zuber, Neutrino–nuclear responses for astro-neutrinos, single beta decays and double beta decays, *Physics Reports* **797**, 1 (2019).
- [62] P. E. Garrett, T. R. Rodríguez, A. D. Varela, K. L. Green, J. Bangay, A. Finlay, R. A. E. Austin, G. C. Ball, D. S. Bandyopadhyay, V. Bildstein, S. Colosimo, D. S. Cross, G. A. Demand, P. Finlay, A. B. Garnsworthy, G. F. Grinyer, G. Hackman, B. Jigmeddorj, J. Jolie, W. D. Kulp, K. G. Leach, A. C. Morton, J. N. Orce, C. J. Pearson, A. A. Phillips, A. J. Radich, E. T. Rand, M. A. Schumaker, C. E. Svensson, C. Sumithrarachchi, S. Triambak, N. Warr, J. Wong, J. L. Wood, and S. W. Yates, Multiple Shape Coexistence in $^{110,112}\text{Cd}$, *Phys. Rev. Lett.* **123**, 142502 (2019).
- [63] P. E. Garrett, T. R. Rodríguez, A. Diaz Varela, K. L. Green, J. Bangay, A. Finlay, R. A. E. Austin, G. C. Ball, D. S. Bandyopadhyay, V. Bildstein, S. Colosimo, D. S. Cross, G. A. Demand, P. Finlay, A. B. Garnsworthy, G. F. Grinyer, G. Hackman, B. Jigmeddorj, J. Jolie, W. D. Kulp, K. G. Leach, A. C. Morton, J. N. Orce, C. J. Pearson, A. A. Phillips, A. J. Radich, E. T. Rand, M. A. Schumaker, C. E. Svensson, C. Sumithrarachchi, S. Triambak, N. Warr, J. Wong, J. L. Wood, and S. W. Yates, Shape coexistence and multiparticle-multipole structures in $^{110,112}\text{Cd}$, *Phys. Rev. C* **101**, 044302 (2020).
- [64] N.J. Stone, Table of nuclear electric quadrupole moments, *Atomic Data and Nuclear Data Tables* **111-112**, 1 (2016).
- [65] N.J. Stone, *Table of Recommended Nuclear Magnetic Dipole Moments: Part I, Long-lived States*, Tech. Rep. INDC(NDS)-0794 (International Atomic Energy Agency, 2019).
- [66] N.J. Stone, *Table of Recommended Nuclear Magnetic Dipole Moments: Part II, Short-lived States*, Tech. Rep. INDC(NDS)-0816 (International Atomic Energy Agency, 2020).
- [67] H. C. Zhang, K. Y. Ma, J. X. Teng, Z. H. Zhao, H. Wang, S. Y. Liu, Y. C. Hao, J. B. Lu, Y. J. Ma, D. Yang, X. G. Wu, Y. Zheng, and C. B. Li, New positive-parity bands in ^{110}Ag and systematic studies in silver isotopes, *Phys. Rev. C* **108**, 024314 (2023).

Supplemental material for "Ultra-low Q_β value for the allowed decay of $^{110}\text{Ag}^m$ confirmed via mass measurements"

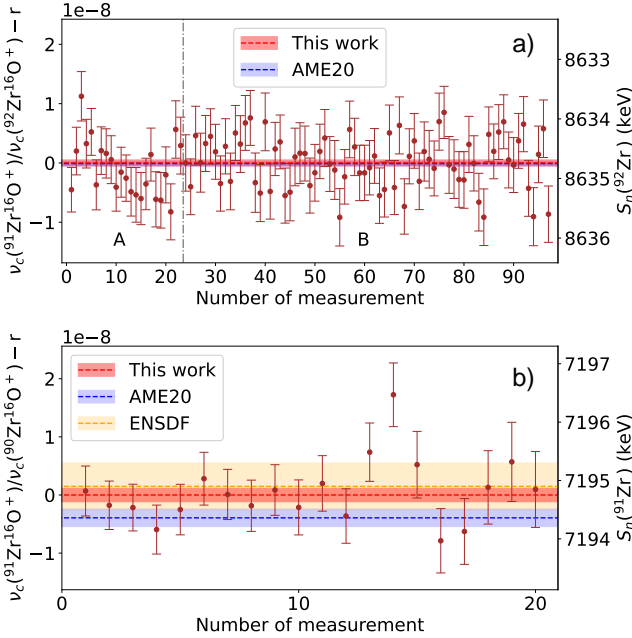


Figure 1. a) Measured frequency ratios $\nu(^{91}\text{Zr}^{16}\text{O}^+)/\nu(^{92}\text{Zr}^{16}\text{O}^+)$ with the gray dotted lines indicating breaks in the measurement and an accumulation time change (A: $t_{\text{acc}} = 1$ s, B: $t_{\text{acc}} = 813$ ms). The magnetron and cyclotron spots for dataset A were collected at an angle of $\alpha_+ \approx \alpha_- \approx 90^\circ$ and for dataset B $\alpha_+ \approx \alpha_- \approx 0^\circ$. The average frequency ratio $r = 1.009\,348\,878\,19(52)$ and the corresponding S_n value for ^{92}Zr are indicated with the red band while the AME20 value [1] is plotted in blue. b) Measured frequency ratios $\nu(^{91}\text{Zr}^{16}\text{O}^+)/\nu(^{90}\text{Zr}^{16}\text{O}^+)$ with accumulation time $t_{\text{acc}} = 1$ s with the magnetron and cyclotron spots at an angle of $\alpha_+ \approx \alpha_- \approx 270^\circ$. The average frequency ratio $r = 0.990\,636\,660\,6(12)$ and the corresponding S_n value for ^{91}Zr are indicated with the red band, the AME20 value [1] is plotted in blue while the ENSDF value [2] based on Ref. [3] in yellow.

Table II. Comparison of the experimental (E_x^{exp}) and theoretical (E_x^{th}) excitation energies of the positive-parity states in ^{110}Ag . The experimental values are taken from Refs. [4, 8].

J^π	E_x^{exp} (keV)	E_x^{th} (keV)
1_{gs}^+	0	0
6_m^+	117.59(5)	207
3_1^+	118.719(10)	20
3_2^+	191.622(12)	319
2_1^+	198.689(10)	259
4_1^+	266.7 ^a	72
5_1^+	379.1 ^a	178
6_2^+	446.89 ^a	276
4_2^+	471.1 ^a	275

^a Exact uncertainties are not given in the reference but are below 1 keV.

Table III. Comparison of the experimental (E_x^{exp}) and theoretical (E_x^{th}) excitation energies of the positive-parity states in ^{110}Cd . The experimental values are taken from Refs. [4, 9].

J^π	E_x^{exp} (keV)	E_x^{th} (keV)
0_{gs}^+	0	0
2_1^+	657.7623(11)	611
0_2^+	1473.07(3)	1493
2_2^+	1475.7900(14)	1546
4_1^+	1542.4441(14)	1583
0_3^+	1731.31(3)	1758
2_3^+	1783.496(15)	1926
4_2^+	1809.48(9)	2205
0_4^+	2078.80(5)	2369
3_1^+	2162.8015(15)	1899
4_3^+	2220.0683(14)	2331
4_4^+	2250.554(11)	2526
2_4^+	2287.63(11)	2027
3_2^+	2433.248(25)	2056
6_1^+	2479.9339(25)	2651
5_1^+	2926.7474(16)	2556
5_2^+	3008.41(4)	2782

Table I. Comparison of the electric quadrupole (Q_s) and magnetic dipole (μ) moments with those computed by the NSM using the $jj45pn$ b Hamiltonian. The experimental values are taken from Refs. [4–7].

Nuclide	J^π	Experimental		Computed	
		Q_s (eb)	μ (μ_N)	Q_s (eb)	μ (μ_N)
^{110}Ag	1_{gs}^+	0.24(12)	2.7225(14)	0.1602	2.6072
^{110}Ag	6_m^+	1.44(10)	3.602(4)	0.8785	3.787
^{110}Ag	3_1^+	–	3.77(3)	0.5815	3.8243
^{110}Cd	2_1^+	-0.40(4)	0.81(6)	-0.32	1.0851

- [1] Meng Wang, W.J. Huang, F.G. Kondev, G. Audi, and S. Naimi, The AME 2020 atomic mass evaluation (II). Tables, graphs and references, *Chinese Physics C* **45**, 030003 (2021).
- [2] C. M. Baglin, Nuclear Data Sheets for $A = 91$, *Nuclear Data Sheets* **114**, 1293 (2013).
- [3] M. A. Lone and G. A. Bartholomew, $^{90}\text{Zr}(n,\gamma)$ Studies with Thermal Neutrons, in *Neutron Capture Gamma-Ray Spectroscopy*, edited by R. E. Chrien and W. R. Kane (Springer US, Boston, MA, 1979) pp. 675–677.
- [4] G. Gürdal and F.G. Kondev, Nuclear Data Sheets for A

- = 110, *Nuclear Data Sheets* **113**, 1315 (2012).
- [5] N.J. Stone, Table of nuclear electric quadrupole moments, *Atomic Data and Nuclear Data Tables* **111-112**, 1 (2016).
- [6] N.J. Stone, *Table of Recommended Nuclear Magnetic Dipole Moments: Part I, Long-lived States*, Tech. Rep. INDC(NDS)-0794 (International Atomic Energy Agency, 2019).
- [7] N.J. Stone, *Table of Recommended Nuclear Magnetic Dipole Moments: Part II, Short-lived States*, Tech. Rep. INDC(NDS)-0816 (International Atomic Energy Agency, 2020).
- [8] H. C. Zhang, K. Y. Ma, J. X. Teng, Z. H. Zhao, H. Wang, S. Y. Liu, Y. C. Hao, J. B. Lu, Y. J. Ma, D. Yang, X. G. Wu, Y. Zheng, and C. B. Li, New positive-parity bands in ^{110}Ag and systematic studies in silver isotopes, *Phys. Rev. C* **108**, 024314 (2023).
- [9] B. Singh, Compiled (unevaluated) dataset from Refs. [10] and [11], compiled on 15 Jun 2020, from XUNDL database as of 01 Sep 2024. Version available at <https://www.nndc.bnl.gov/xndlarchivals/>.
- [10] P. E. Garrett, T. R. Rodríguez, A. D. Varela, K. L. Green, J. Bangay, A. Finlay, R. A. E. Austin, G. C. Ball, D. S. Bandyopadhyay, V. Bildstein, S. Colosimo, D. S. Cross, G. A. Demand, P. Finlay, A. B. Garnsworthy, G. F. Grinyer, G. Hackman, B. Jigmeddorj, J. Jolie, W. D. Kulp, K. G. Leach, A. C. Morton, J. N. Orce, C. J. Pearson, A. A. Phillips, A. J. Radich, E. T. Rand, M. A. Schumaker, C. E. Svensson, C. Sumithrarachchi, S. Triambak, N. Warr, J. Wong, J. L. Wood, and S. W. Yates, Multiple Shape Coexistence in $^{110,112}\text{Cd}$, *Phys. Rev. Lett.* **123**, 142502 (2019).
- [11] P. E. Garrett, T. R. Rodríguez, A. Diaz Varela, K. L. Green, J. Bangay, A. Finlay, R. A. E. Austin, G. C. Ball, D. S. Bandyopadhyay, V. Bildstein, S. Colosimo, D. S. Cross, G. A. Demand, P. Finlay, A. B. Garnsworthy, G. F. Grinyer, G. Hackman, B. Jigmeddorj, J. Jolie, W. D. Kulp, K. G. Leach, A. C. Morton, J. N. Orce, C. J. Pearson, A. A. Phillips, A. J. Radich, E. T. Rand, M. A. Schumaker, C. E. Svensson, C. Sumithrarachchi, S. Triambak, N. Warr, J. Wong, J. L. Wood, and S. W. Yates, Shape coexistence and multiparticle-multiparticle structures in $^{110,112}\text{Cd}$, *Phys. Rev. C* **101**, 044302 (2020).